Histol Histopathol (2009) 24: 1531-1540

**http://www.hh.um.es**

**Histology and Histopathology**

*Cellular and Molecular Biology*

# Comparison of the effect of cryopreservation protocols on the histology of bioengineered tissues

**Deyanira Serrato[1], Renato Nieto-Aguilar[1], Ingrid Garzón[1], Olga Roda[2], Antonio Campos[1] and Miguel Alaminos[1]**

[1]Tissue Engineering Group, Department of Histology, University of Granada, Spain and [2]Department of Human Anatomy and Embryology, University of Granada, Granada, Spain

**Summary.** The purpose of this study was to compare the effects of five different cryopreservation protocols on the histology of bioengineered tissues. Although several artificial tissues have been developed to the date by tissue engineering, classical histological analysis methods and techniques must be optimized for these new tissues with special properties. The results of this study showed that the use of volatile solutions (formaldehyde, glutaraldehyde, glacial acetic acid and acetone) was not able to prevent the formation of large ice crystals that, in turn, can alter the structure of the artificial tissues. However, preincubation of the tissues in different concentrations of a carbon hydrate (glucose, maltose or trehalose) resulted in a better preservation of the tissue structure. We conclude that the best protocol that allows for an efficient analysis of the bioengineered tissues with very few artifacts is preincubation of the tissues in 0.300M or 0.400M trehalose for 30 or 120 min prior to *OCT* (optimal cutting temperature) embedding and cryosectioning. For all those reasons, we recommend the use of a cryoprotective agent before *OCT* embedding of human artificial tissues.

**Key words:** Tissue engineering, Methods, Histological analysis, Cryosection, Fibrin-agarose constructs

## Introduction

Construction of artificial organs by tissue engineering is one of the research fields that has experienced major progress during recent years (Atala, 2000). By using tissue engineering techniques, several researchers have developed different artificial organs and tissues with therapeutic potential using diverse biomaterials as stroma substitutes. Biomaterials should imitate, in most part, the extracellular matrix of the desired structure and organ function (Li et al., 2002; Boland et al., 2004), including adequate resistance and support (Bruder and Fox, 1999), control of bioactive molecule liberation, biocompatibility and biodegradable properties (Hutmacher et al., 2001).

In this regard, our research group has developed a novel stromal substitute made of a mixture of human fibrin and agarose type VII that has demonstrated appropriate biomechanical and structural properties when used for tissue engineering purposes, including the successful generation of oral mucosa and corneas (Alaminos et al., 2006, 2007; Sanchez-Quevedo et al., 2007). Once the artificial substitutes are generated, histological analysis is an important part of the evaluation process and quality control of the artificial tissues developed by tissue engineering. Moreover, histological analysis technique has to be accurate and sensitive and the image obtained under the microscope must be real and free from artifacts.

In this context, one of the most rapid techniques that allows an efficient preservation of most of the protein epitopes to facilitate proteomic analysis, such as immunological assays, is the cryoprocessing of tissues embedded in *OCT* (optimal cutting temperature) (Naber et al., 1992; Rahimi et al., 2006). Cryoprocessing of tissue samples embedded in *OCT* has several advantages over paraffin embedding, especially the rapidness of the procedure and the maintenance of the structure and biochemical composition of the tissue. However, *OCT* technique must be optimized for certain tissue types that have high contents of water and low physical resistance to strength, as is the case of tissues generated in the laboratory by tissue engineering. For that reason, the use of cryotechniques could generate false histological images with a high number of artifacts, mainly due to

*Offprint requests to:* Miguel Alaminos, University of Granada, Faculty of Medicine, Avenida de Madrid 11, E18012 Granada, Spain. e-mail: malaminos@ugr.es

the formation of large crystals of ice that, in turn, may alter or even destroy the structure of the bioengineered tissue.

To avoid the formation of large water crystals, the use of certain cryoprotective agents has been suggested (Barthel and Raymond, 1990; Naber et al., 1992; Loken and Demetrick, 2005). For that reason, in this work, we have carried out a cryostat histological analysis on human tissue substitutes developed by tissue engineering using different cryofixation protocols in order to identify an accurate method for the analysis of this kind of artificial tissue.

## Materials and methods

### *Fabrication of fibrin-agarose tissue constructs*

Human fibrin was obtained from frozen plasma of human blood donors (kindly provided by Dr. Fernandez-Montoya, Human Tissue Bank of Granada). To produce a scaffold by tissue engineering (Alaminos et al., 2006, 2007; Sanchez-Quevedo et al., 2007) 21 ml of human plasma were added to 2 ml of DMEM with 10% FCS. To prevent degradation of the scaffold by fibrinolysis, the mixture was supplemented with 200 µl of tranexamic acid. Then, 2 ml of 1% $CaCl_2$ were added to the solution to precipitate fibrin polymerization. Finally, type VII agarose was melted and dissolved in PBS and added to the fibrin mixture at a final concentration of 0.1%, immediately after the $CaCl_2$ was added. The mixture was seeded in Petri dishes and allowed to solidify at 37°C for 2 hours.

### *Cryoprotection protocols for histological analysis of fibrin-agarose scaffolds*

Fibrin-agarose scaffolds were cut into small pieces of approximately 0.5x0.5x0.25 cm and each piece was preincubated in a different cryoprotective agent for different times before being embedded in *OCT* compound (Tissue-Tek) and cryofixed at liquid nitrogen temperature. *OCT* compound is a formulation of water-soluble glycols and resins, providing a convenient specimen matrix for cryostat sectioning at temperatures of -10°C and below. As a control, one group of samples was fixed for 2 h in 4% formalin and embedded in paraffin following standard procedures. Briefly, fixed samples were washed in water and dehydrated in graded ethanol series (50, 70, 96 and 100%). Then, the ethanol was substituted by toluene and the samples were cleared three times in xylene. Finally, samples were included in liquid paraffin and 4 µm sections were obtained using a microtome.

The specific groups of study included in this work are the following: 1) samples included in *OCT* without any previous cryoprotective procedure. 2) samples preincubated in a volatile agent (acetone, acetic acid, formaldehyde or glutaraldehyde) for 60 min before *OCT* embedding. 3) samples preincubated in a 0.002M, 0.020M, 0.050M, 0.080M, 0.100M, 0.200M, 0.300M or 0.400M solution of glucose for 30, 60 or 120 min before *OCT* embedding. 4) samples preincubated in a 0.002M, 0.020M, 0.050M, 0.080M, 0.100M, 0.200M, 0.300M or 0.400M solution of maltose for 30, 60 or 120 min before *OCT* embedding. 5) samples preincubated in a 0.002M, 0.020M, 0.050M, 0.080M, 0.100M, 0.200M, 0.300M or 0.400M solution of trehalose for 30, 60 or 120 min before *OCT* embedding. Three different tissue samples were incubated in each group of study.

The concentration used for acetone and acetic acid was 100%, whereas formaldehyde was used at 4% and glutaraldehyde concentration was 3%. All concentrations of glucose, maltose and trehalose were prepared in distilled water at room temperature.

Once incubated in the different cryoprotective solutions, all samples were embedded in *OCT* compound (Sakura Finetek USA) and cryofixed at liquid nitrogen temperature. Then, five micron-sections were obtained by using a cryostat microtome at -20º C, placed on microscope slides and stained with hematoxylin and eosin using standard methods. Finally, the structure of the artificial tissues was evaluated by quantifying the average area and diameter of the interfibrillar spaces generated within the fiber mesh using the software NIS-AR 301E with an ECLIPSE Ti light microscope (Nikon Ltd., Tokio, Japan). In brief, 10 images were taken from each sample using 200x magnifications, and all spaces allocated within the artificial tissues were detected using the automatic mode of the software. This software allows for the automatic identification of all empty spaces in each image and, therefore, the possibility of errors or biases is minimized. Once detected, the area and diameter of 10 spaces were calculated for each image. Average area and diameter of all spaces analyzed in this work were 6938.6 $\mu m^2$ and 69.3 µm, respectively.

### *Statistical analysis*

To compare the average areas and diameters of the samples submitted to each cryopreservation protocol with the control paraffin-embedded tissues, we used the non-parametric test U of Mann-Whitney. For each comparison, a Bonferroni-adjusted two-sided significance level of 0.001 was considered, because up to more than 50 statistical tests were used at the same time. Comparisons with p value of 0.001 were considered as marginally significant, whereas values higher than 0.001 were considered as non-significant. To carry out the previously described statistical analysis, we used SPSS 13.0 software.

## Results

### *Histological analysis of formalin-fixed paraffin-embedded control samples*

As controls, artificial tissues were fixed in formalin and embedded in paraffin. The use of this standard

technique showed good results, with proper preservation of the structure and architecture of the fiber mesh of the artificial matrix (Fig. 1A), allowing for an adequate sectioning and staining of the artificial tissues. The mean area and diameter of the spaces that appeared among the mesh fibers of the artificial tissues were very small, with 44.4±25.2 $\mu m^2$ and 7.2±2.3 µm, respectively (Table 1).

### *Histological analysis of untreated, OCT-embedded artificial tissues*

The structure and architecture of the artificial tissue observed with this procedure showed poor results, characterized by a disorganization of the fiber mesh and the presence of holes, gaps and fissures among the mesh fibers, with a mean area of 8557.7±7273.9 $\mu m^2$ and a mean diameter of 95.5±44.4 µm, much higher than that observed in formalin-fixed, paraffin-embedded control tissues ($p<0.001$). In addition, sample cryosectioning was difficult to perform, and generation of 5 µm-thickness sections of these tissues was complicated due to a loose consistency of the tissues (Fig. 1B).

### *Histological analysis of samples pretreated with acetone, glacial acetic acid, formaldehyde or glutaraldehyde and embedded in OCT*

Artificial tissues pretreated with acetone, glacial acetic acid, formalin or glutaraldehyde and embedded in *OCT* at liquid nitrogen temperature, were difficult to manage using the cryostat. In fact, generation of 5 µm-thickness cryosections of these tissues was very complicated due to the lack of consistency of these tissues. Furthermore, the artificial tissues were highly disorganized, with the presence of large holes, gaps and fissures whose areas were 322.5, 453.9, 356.7 and 368.1 times higher in comparison with the formalin-fixed, paraffin-embedded tissues (Table 1). Differences were statistically significant for both the area and the diameter of the artificial tissues ($p<0.001$). Illustrative examples of bioengineered tissues processed with these techniques are shown in Figure 1 C-F.

### *Histological analysis of samples pretreated with glucose, maltose or trehalose and embedded in OCT*

Glucose

In the first place, artificial tissues incubated in 0.002M, 0.020M, 0.050M, 0.080M, 0.100M, 0.200M, 0.300M and 0.400M glucose as a cryoprotective solution for 30 min had very low consistency, with high spaces

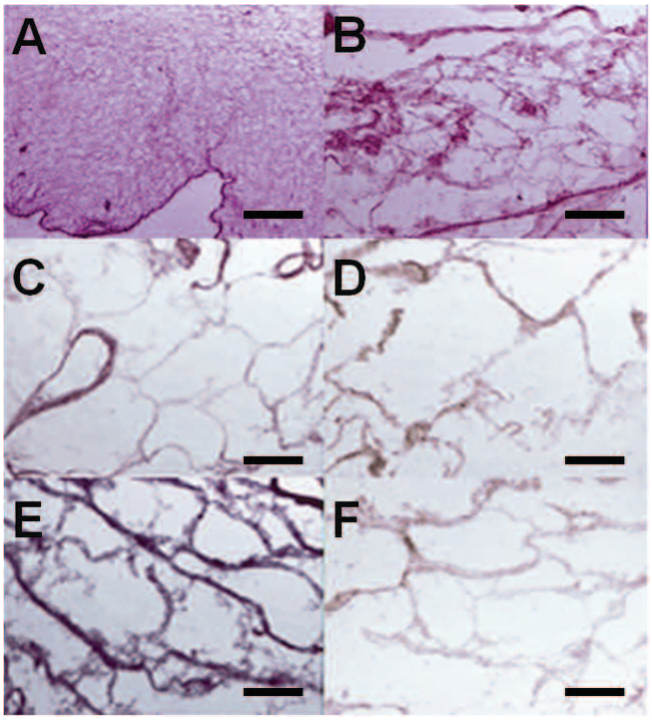


**Fig. 1.** Histological analysis of formalin-fixed paraffin-embedded bioengineered human tissues -control samples- **(A)**, tissues embedded in *OCT* without any previous treatment **(B)**, samples pretreated with acetone **(C)**, glacial acetic acid **(D)**, formaldehyde **(E)** or glutaraldehyde **(F)** and embedded in OCT. H&E staining. Scale bars: 1 µm.

**Table 1.** Results of the histological analysis of formalin-fixed paraffin-embedded human control artificial tissues, samples embedded in *OCT* without previous cryoprotection and bioengineered tissues preincubated in different volatile agents for different times and embedded in *OCT*.

| Preincubation solution | Average area | Average diameter | Standard deviation area | Standard deviation diameter | Fold-change area | Fold-change diameter | Area p value vs. control | Diameter p value vs. control |
|---|---|---|---|---|---|---|---|---|
| Paraffin-Embedding (Control) | 44.4 | 7.2 | 25.2 | 2.3 | 1.0 | 1.0 | - | - |
| No Peincubation (*OCT* only) | 8557.7 | 95.5 | 7273.9 | 44.4 | 192.7 | 13.3 | 0.000 | 0.000 |
| Acetone | 14320.5 | 130.8 | 7392.3 | 35.3 | 322.5 | 18.2 | 0.000 | 0.000 |
| Glacial Acetic Acid | 20155.2 | 145.5 | 21185.1 | 70.7 | 453.9 | 20.2 | 0.000 | 0.000 |
| Formaldehyde | 15841.3 | 138.1 | 8017.4 | 35.1 | 356.7 | 19.2 | 0.000 | 0.000 |
| Glutarhaldehyde | 16344.1 | 141.0 | 7528.8 | 32.1 | 368.1 | 19.6 | 0.000 | 0.000 |

The average area and diameter correspond to the interfibrillar spaces that appear in the fiber mesh after cryosectioning and staining. Fold-change area corresponds to the ratio of the average area for each specific condition versus area of the paraffin-embedded control tissues. Fold-change diameter corresponds to the ratio of the average diameter for each specific condition versus diameter of the paraffin-embedded control tissues.

among the mesh fibers, whose areas ranged between 15094.2±6361.4 $\mu m^2$ and 22529.2±94.8 $\mu m^2$, and whose diameters ranged between 84.8±18.6 µm and 116.5±42.5 µm, with an average area and diameter of 17737.7±2674.9 $\mu m^2$ and 137.4±3.9 µm respectively. Statistical comparison of both the areas and diameters of tissues pretreated with glucose for 30 min with the control samples showed statistically significant differences for all concentrations ($p<0.001$).

Secondly, when the tissues were incubated in different glucose solutions for 60 min, we found that the consistency of the tissues was appropriate when 0.200M, 0.300M or 0.400M glucose was used, being very low for lower concentrations of glucose. Average area and diameter of the spaces found in the artificial tissues incubated for 60 min in the different concentrations of glucose were 12206.9±3187.6 $\mu m^2$ and 114.6±15.1 µm respectively, ranging between 6920.2±6669.9 $\mu m^2$ and 16875.9±14345.9 $\mu m^2$ for the area, and between 87.3±36.5 µm and 134.9±60.5 µm for the diameter. Differences with the control samples were statistically significant for all concentrations ($p<0.001$).

Finally, when the tissues were incubated for 120 min, we found that the consistency of the tissues was appropriate when 0.100M, 0.200M, 0.300M or 0.400M glucose was used, being very low for lower concentrations of glucose. The average area and diameter of the spaces in the different concentrations of glucose 120 min were 7905.2 $\mu m^2$ and 94.3 µm respectively, ranging between 5895.6±2242.3 $\mu m^2$ and 11928.3±10423.4 $\mu m^2$ for the area, and between 84.8±15.7µm and 116.4±50.5 µm for the diameter. Differences with the control samples were statistically significant at all concentrations of glucose ($p<0.001$) (Table 2). Ilustrative examples of bioengineered tissues processed with these techniques are shown in Figure 2.

Maltose

When the artificial tissues were incubated in different maltose solutions for 30 min, we found that the consistency of the tissues was appropriate when 0.080M, 0.100M, 0.200M, 0.300M and 0.400M maltose was used, being very low for lower concentrations of maltose. In general, samples presented middle-size and smaller spaces among the mesh fibers whose areas ranged between 91.8±74.2 $\mu m^2$ and 9460.2±12255.0 $\mu m^2$, and whose diameters ranged between 9.9±4.3 µm and 108.7±57.5 µm, with an average area and diameter of 3402.5±3724.2 $\mu m^2$ and 51.2±34.5 µm respectively. Statistical comparison of both the areas and diameters of tissues pretreated with maltose for 30 min with the

**Table 2.** Results of the histological analysis of human artificial tissues preincubated in different concentrations of glucose for different times and embedded in *OCT*.

| Preincubation time | Preincubation concentration | Average area (µm2) | Average diameter (µm) | Standard deviation area | Standard deviation diameter | Fold-change area | Fold-change diameter | Area p value vs. control | Diameter p value vs. control |
|---|---|---|---|---|---|---|---|---|---|
| 30 min | 0.002M | 16665.6 | 139.8 | 10575.7 | 43 | 375.3 | 19.4 | 0.000 | 0.000 |
| | 0.020M | 16892.3 | 134.8 | 16745.9 | 61 | 380.4 | 18.7 | 0.000 | 0.000 |
| | 0.050M | 16522.1 | 135.7 | 11575.3 | 54.1 | 372.1 | 18.8 | 0.000 | 0.000 |
| | 0.080M | 21380 | 134.2 | 27634.5 | 101.2 | 481.5 | 18.6 | 0.000 | 0.000 |
| | 0.100M | 16401.3 | 133.6 | 12035.7 | 58.1 | 369.4 | 18.5 | 0.000 | 0.000 |
| | 0.200M | 22529.2 | 143.5 | 28962.7 | 94.8 | 507.4 | 19.9 | 0.000 | 0.000 |
| | 0.300M | 15094.2 | 135.8 | 6361.4 | 29.5 | 339.9 | 18.9 | 0.000 | 0.000 |
| | 0.400M | 16416.6 | 142.2 | 6318.7 | 27.7 | 369.7 | 19.7 | 0.000 | 0.000 |
| 60 min | 0.002M | 15636.6 | 129.8 | 14769.9 | 58.4 | 352.1 | 18 | 0.000 | 0.000 |
| | 0.020M | 16875.9 | 134.9 | 14345.9 | 60.5 | 380 | 18.7 | 0.000 | 0.000 |
| | 0.050M | 11516.3 | 114 | 8975.5 | 43.2 | 259.3 | 15.8 | 0.000 | 0.000 |
| | 0.080M | 13929.5 | 123.7 | 11251.5 | 51.9 | 313.7 | 17.2 | 0.000 | 0.000 |
| | 0.100M | 11574.8 | 108.9 | 12542.4 | 56.5 | 260.7 | 15.1 | 0.000 | 0.000 |
| | 0.200M | 10048.2 | 105.5 | 8460.7 | 42.9 | 226.3 | 14.7 | 0.000 | 0.000 |
| | 0.300M | 11153.4 | 112.6 | 7949 | 41.1 | 251.2 | 15.6 | 0.000 | 0.000 |
| | 0.400M | 6920.2 | 87.3 | 6669.9 | 36.5 | 155.8 | 12.1 | 0.000 | 0.000 |
| 120 min | 0.002M | 10295.2 | 104 | 10423.4 | 50.5 | 231.8 | 14.4 | 0.000 | 0.000 |
| | 0.020M | 11928.3 | 116.5 | 9143.5 | 42.5 | 268.6 | 16.2 | 0.000 | 0.000 |
| | 0.050M | 7123.4 | 87.8 | 6235.6 | 38.8 | 160.4 | 12.2 | 0.000 | 0.000 |
| | 0.080M | 7011.7 | 92.1 | 3428 | 22 | 157.9 | 12.8 | 0.000 | 0.000 |
| | 0.100M | 7298.4 | 91.5 | 5058.9 | 31.9 | 164.4 | 12.7 | 0.000 | 0.000 |
| | 0.200M | 6114.6 | 87 | 2242.4 | 15.7 | 137.7 | 12.1 | 0.000 | 0.000 |
| | 0.300M | 5895.7 | 84.8 | 2520.7 | 18.6 | 132.8 | 11.8 | 0.000 | 0.000 |
| | 0.400M | 7574.7 | 91.5 | 6105.3 | 37.7 | 170.6 | 12.7 | 0.000 | 0.000 |

The average area and diameter correspond to the interfibrillar spaces that appear in the fiber mesh after cryosectioning and staining. Fold-change area corresponds to the ratio of the average area for each specific condition versus area of the paraffin-embedded control tissues. Fold-change diameter corresponds to the ratio of the average diameter for each specific condition versus diameter of the paraffin-embedded control tissues.

control samples showed statistically significant differences for all concentrations ($p<0.001$) except for 0.300M and 0.400M ($p>0.001$), being marginally significant for 0.080M ($p=0.001$).

Secondly, when the tissues were incubated in different maltose solutions for 60 min, we found that the consistency of the tissues was appropriate when maltose 0.080M, 0.100M, 0.200M, 0.300M and 0.400M was used, being very low for 0.050, 0.020 and 0.002. Average area and diameter of the spaces found in the artificial tissues incubated for 60 min in the different concentrations of maltose were 7771.8±7225.8 $\mu m^2$ and 81.2±43.9 µm respectively. Spaces found in samples incubated in maltose for 60 min ranged between 537.3±515.2 $\mu m^2$ and 21923.7±16473.2 $\mu m^2$ for the area, and between 23.8±11.2 µm and 158.2±70.4 µm for the diameter. Differences with the control samples were statistically significant ($p<0.001$).

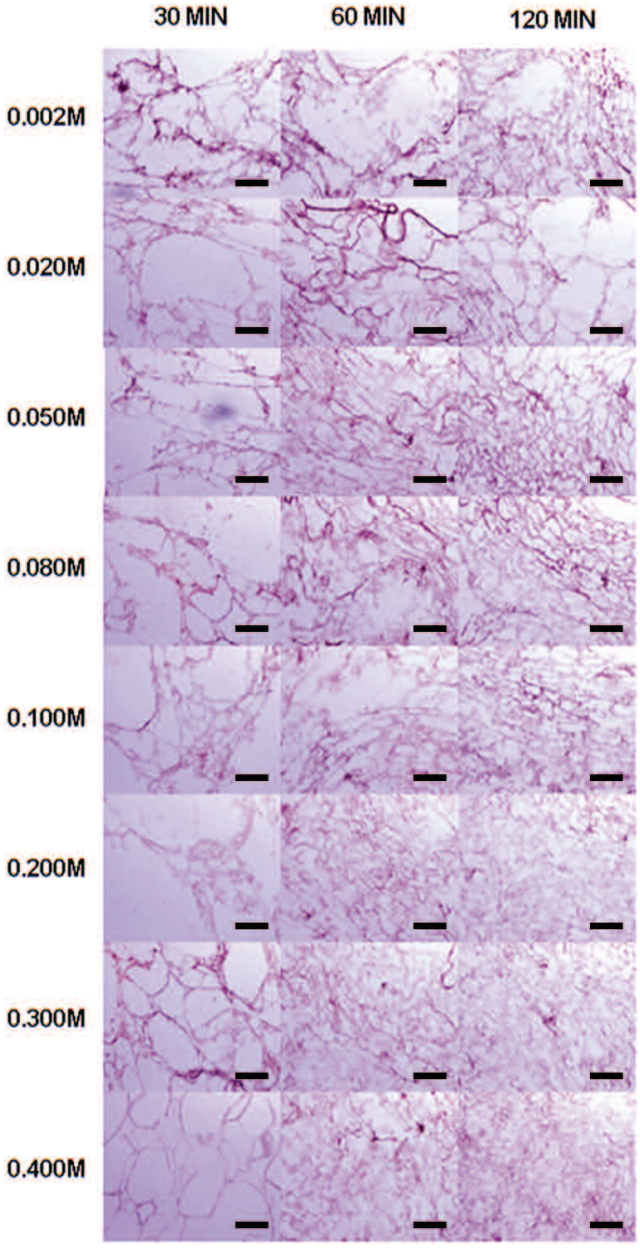


**Fig. 2.** Histological analysis of bioengineered human tissues preincubated in different concentrations of glucose for 30, 60 or 120 min and embedded in *OCT* for cryosectioning and H&E staining. Scale bars: 1 µm.

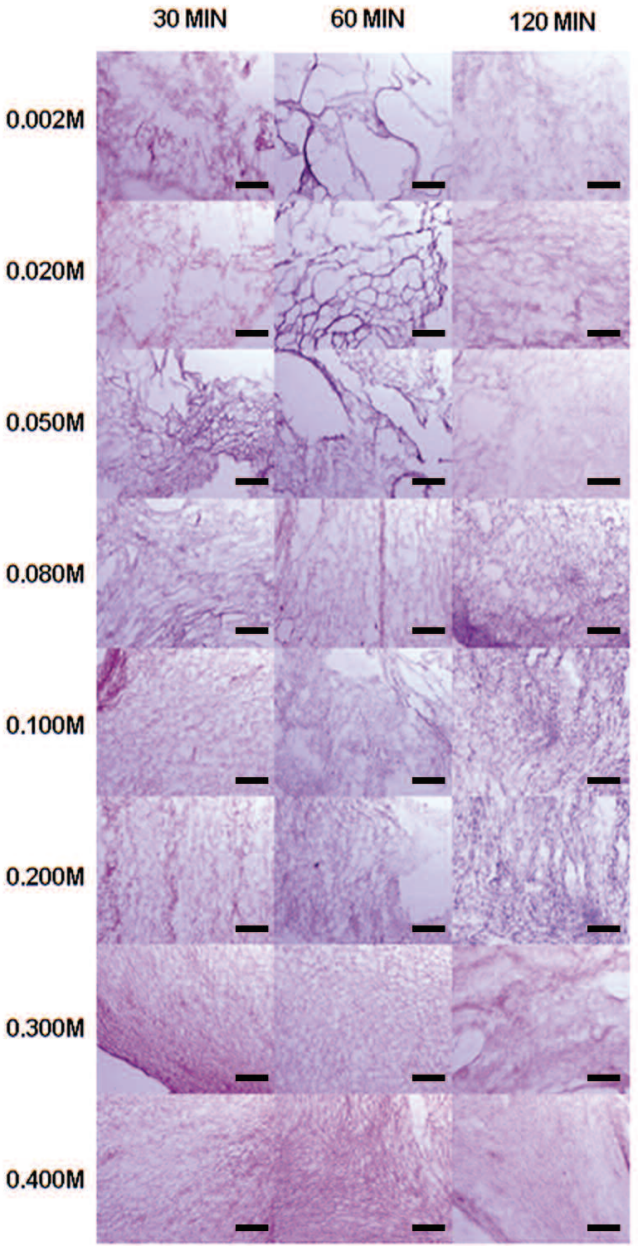


**Fig. 3.** Histological analysis of bioengineered human tissues preincubated in different concentrations of maltose for 30, 60 or 120 min and embedded in *OCT* for cryosectioning and H&E staining. Scale bars: 1 µm.

Finally, when the tissues were incubated in different maltose solutions for 120 min, the consistency of the tissues was higher than for the tissues incubated in maltose for 30 or 60 min, allowing cryosectioning and mounting on microscope slides. Average area and diameter of the spaces found in the artificial mesh of the tissues incubated for 120 min were 1432.5±1392.0 $\mu m^2$ and 33.3±18.6 µm, respectively, ranging between 135.5±178.4 $\mu m^2$ and 4040.7±4776.2 $\mu m^2$ for the area, and between 10.9±7.7µm and 62.9±36.1 µm for the diameter. Differences with the control samples were statistically significant ($p<0.001$) for samples incubated in 0.002M, 0.020M, 0.050M and 0.080M, but not for higher concentrations ($p>0.001$) (Table 3). llustrative examples of bioengineered tissues preincubated in maltose are shown in Figure 3.

Trehalose

Bioengineered human tissues incubated in trehalose 0.002M or 0.020M solutions for 30 min had very low consistency, which was inappropriate for cryosection. However, samples incubated in 0.050M, 0.080M, 0.100M, 0.200M, 0.300M or 0.400M trehalose for 30 min had proper consistency and were correctly sectioned. In general, samples presented small spaces among the fiber mesh, whose mean area ranged between 33.4±34.0 $\mu m^2$ and 4394.3.±6714.4 $\mu m^2$ and whose diameter ranged between 5.8±3.0 µm and 54.5±54.0 µm. Average area and diameter were 1069.4±1526.3 $\mu m^2$ and 22.6±17.8 µm, respectively (Fig. 5). Statistical comparisons of both the areas and diameters of tissues pretreated with trehalose for 30 min with the control samples did not show any statistically significant differences (p 0.001).

Secondly, when the tissues were incubated in trehalose for 60 min, we found that the consistency of the tissues was appropriate for cryosectioning procedures at all concentrations. Average area and diameter of the spaces found in the artificial tissues incubated for 60 min in the different concentrations of trehalose were 1023.7±1316.7 $\mu m^2$ and 26.7±17.0 µm, respectively, ranging between 127.4±107.7 $\mu m^2$ and 3758.3±4385.9 $\mu m^2$ for the area, and 60.3±35.6 µm and 11.7±5.1 µm for the diameter. Differences with the control samples were statistically significant for 0.002M and 0.020M trehalose ($p<0.001$), but not for higher concentrations of trehalose.

Finally, when the tissues were incubated in different trehalose solutions for 120 min, we found that the consistency of the tissues was high, allowing for cryosection, although the tissues became very hard and

**Table 3.** Results of the histological analysis of human artificial tissues preincubated in different concentrations of maltose for different times and embedded in *OCT*.

| Preincubation time | Preincubation concentration | Average area (µm2) | Average diameter (µm) | Standard deviation area | Standard deviation diameter | Fold-change area | Fold-change diameter | Area p value vs. control | Diameter p value vs. control |
|---|---|---|---|---|---|---|---|---|---|
| 30 min | 0.002M | 9460.3 | 108.7 | 2899.3 | 15.6 | 213.0 | 15.1 | 0.000 | 0.000 |
| | 0.020M | 9081.7 | 92.7 | 12255.0 | 57.5 | 204.5 | 12.9 | 0.000 | 0.000 |
| | 0.050M | 2255.6 | 44.6 | 3116.8 | 31.3 | 50.8 | 6.2 | 0.000 | 0.000 |
| | 0.080M | 2004.3 | 45.1 | 1744.1 | 24.1 | 45.1 | 6.3 | 0.000 | 0.000 |
| | 0.100M | 2006.5 | 50.1 | 555.7 | 7.3 | 45.2 | 7.0 | 0.000 | 0.000 |
| | 0.200M | 2135.6 | 46.3 | 2138.0 | 25.3 | 48.1 | 6.4 | 0.000 | 0.000 |
| | 0.300M | 184.9 | 12.6 | 274.7 | 9.2 | 4.2 | 1.8 | 0.000 | 0.000 |
| | 0.400M | 91.8 | 10.0 | 74.2 | 4.4 | 2.1 | 1.4 | 0.000 | 0.000 |
| 60 min | 0.002M | 21923.7 | 158.2 | 14291.7 | 56.6 | 493.7 | 22.0 | 0.000 | 0.000 |
| | 0.020M | 11254.2 | 109.2 | 12356.0 | 51.7 | 253.4 | 15.2 | 0.000 | 0.000 |
| | 0.050M | 12612.3 | 107.7 | 16473.2 | 70.4 | 284.0 | 15.0 | 0.000 | 0.000 |
| | 0.080M | 5277.4 | 77.2 | 3899.4 | 29.0 | 118.8 | 10.7 | 0.000 | 0.000 |
| | 0.100M | 6833.9 | 85.0 | 5666.4 | 40.6 | 153.9 | 11.8 | 0.000 | 0.000 |
| | 0.200M | 2367.2 | 50.2 | 2541.6 | 23.3 | 53.3 | 7.0 | 0.000 | 0.000 |
| | 0.300M | 1368.4 | 38.9 | 1264.9 | 16.0 | 30.8 | 5.4 | 0.000 | 0.000 |
| | 0.400M | 537.4 | 23.9 | 515.2 | 11.3 | 12.1 | 3.3 | 0.000 | 0.000 |
| 120 min | 0.002M | 4040.7 | 63.0 | 4776.3 | 36.2 | 91.0 | 8.7 | 0.000 | 0.000 |
| | 0.020M | 2494.4 | 47.3 | 3358.3 | 32.3 | 56.2 | 6.6 | 0.000 | 0.000 |
| | 0.050M | 2317.2 | 49.8 | 2341.6 | 22.9 | 52.2 | 6.9 | 0.000 | 0.000 |
| | 0.080M | 1082.5 | 32.2 | 1335.7 | 19.4 | 24.4 | 4.5 | 0.000 | 0.000 |
| | 0.100M | 835.9 | 29.5 | 808.6 | 14.8 | 18.8 | 4.1 | 0.063 | 0.063 |
| | 0.200M | 376.7 | 21.0 | 224.9 | 6.6 | 8.5 | 2.9 | 0.035 | 0.035 |
| | 0.300M | 177.3 | 13.1 | 197.2 | 7.8 | 4.0 | 1.8 | 0.063 | 0.063 |
| | 0.400M | 135.5 | 10.9 | 178.4 | 7.7 | 3.1 | 1.5 | 0.529 | 0.529 |

The average area and diameter correspond to the interfibrillar spaces that appear in the fiber mesh after cryosectioning and staining. Fold-change area corresponds to the ratio of the average area for each specific condition versus area of the paraffin-embedded control tissues. Fold-change diameter corresponds to the ratio of the average diameter for each specific condition versus diameter of the paraffin-embedded control tissues.

**Table 4.** Results of the histological analysis of human artificial tissues preincubated in different concentrations of trehalose for different times and embedded in *OCT*.

| Preincubation time | Preincubation concentration | Average area (μm2) | Average diameter (μm) | Standard deviation area | Standard deviation diameter | Fold-change area | Fold-change diameter | Area p value vs. control | Diameter p value vs. control |
|---|---|---|---|---|---|---|---|---|---|
| 30 min | 0.002M | 4394.4 | 54.5 | 6714.4 | 54.0 | 99.0 | 7.6 | 0.001 | 0.001 |
| | 0.020M | 2005.6 | 38.9 | 2535.5 | 33.9 | 45.2 | 5.4 | 0.089 | 0.089 |
| | 0.050M | 1392.6 | 34.3 | 1819.6 | 25.7 | 31.4 | 4.8 | 0.001 | 0.001 |
| | 0.080M | 343.6 | 15.8 | 538.7 | 14.4 | 7.7 | 2.2 | 0.315 | 0.315 |
| | 0.100M | 114.0 | 9.8 | 173.6 | 7.5 | 2.6 | 1.4 | 0.739 | 0.739 |
| | 0.200M | 226.4 | 15.4 | 193.9 | 7.6 | 5.1 | 2.1 | 0.009 | 0.009 |
| | 0.300M | 45.7 | 6.8 | 52.6 | 3.7 | 1.0 | 0.9 | 0.393 | 0.393 |
| | 0.400M | 33.4 | 5.8 | 34.1 | 3.1 | 0.8 | 0.8 | 0.280 | 0.280 |
| 60 min | 0.002M | 3758.3 | 60.3 | 4386.0 | 35.7 | 84.6 | 8.4 | 0.000 | 0.000 |
| | 0.020M | 2366.5 | 45.7 | 3311.3 | 32.0 | 53.3 | 6.3 | 0.000 | 0.000 |
| | 0.050M | 497.1 | 23.3 | 453.1 | 10.1 | 11.2 | 3.2 | 0.004 | 0.004 |
| | 0.080M | 364.0 | 17.3 | 472.6 | 13.5 | 8.2 | 2.4 | 0.035 | 0.035 |
| | 0.100M | 448.9 | 19.5 | 589.6 | 14.6 | 10.1 | 2.7 | 0.029 | 0.029 |
| | 0.200M | 338.0 | 19.8 | 203.7 | 6.5 | 7.6 | 2.8 | 0.075 | 0.075 |
| | 0.300M | 127.4 | 11.8 | 107.7 | 5.2 | 2.9 | 1.6 | 0.043 | 0.043 |
| | 0.400M | 289.6 | 16.1 | 377.3 | 11.0 | 6.5 | 2.2 | 0.023 | 0.023 |
| 120 min | 0.002M | 3707.5 | 56.7 | 4988.5 | 40.9 | 83.5 | 7.9 | 0.000 | 0.000 |
| | 0.020M | 1039.2 | 31.1 | 1188.6 | 20.0 | 23.4 | 4.3 | 0.000 | 0.000 |
| | 0.050M | 1191.0 | 28.9 | 2000.9 | 27.5 | 26.8 | 4.0 | 0.001 | 0.001 |
| | 0.080M | 1435.1 | 38.6 | 1197.0 | 19.4 | 32.3 | 5.4 | 0.000 | 0.000 |
| | 0.100M | 1197.5 | 26.3 | 2861.6 | 30.4 | 27.0 | 3.7 | 0.011 | 0.011 |
| | 0.200M | 1044.3 | 31.7 | 1198.5 | 18.9 | 23.5 | 4.4 | 0.000 | 0.000 |
| | 0.300M | 157.3 | 10.3 | 314.6 | 10.2 | 3.5 | 1.4 | 0.971 | 0.971 |
| | 0.400M | 21.9 | 5.1 | 10.8 | 1.3 | 0.5 | 0.7 | 0.029 | 0.029 |

The average area and diameter correspond to the interfibrillar spaces that appear in the fiber mesh after cryosectioning and staining. Fold-change area corresponds to the ratio of the average area for each specific condition versus area of the paraffin-embedded control tissues. Fold-change diameter corresponds to the ratio of the average diameter for each specific condition versus diameter of the paraffin-embedded control tissues.

cryosection was not easy. Average area and diameter of the spaces found in the artificial tissues incubated for 120 min in trehalose were 1224.2±1125.2 $\mu m^2$ and 28.6±16.0 μm respectively, ranging between 21.9±10.8 $\mu m^2$ and 3707.4±4988.4 $\mu m^2$ for the area, and 5.1±1.3μm and 56.7±40.8 μm for the diameter (Fig. 5). Differences with the control samples were statistically significant for 0.002M, 0.020M, 0.080M and 0.200M trehalose ($p<0.001$) and marginally significant for 0.001M ($p=0.001$). No differences were found for the rest of the concentrations of trehalose (Table 4). Illustrative examples of the histological analysis of artificial tissues preincubated in trehalose solutions are shown in Figure 4.

## Discussion

Construction of artificial tissues by tissue engineering is a novel technique that allows for the *in vitro* development of all kinds of human tissues with potential clinical usefulness. Among others, different researchers have reported the efficient creation of oral mucosa, cornea, skin, cartilage, bone and muscle using different biomaterials as stromal substitutes (Alaminos et al., 2006, 2007; Moharamzadeh et al., 2007; Sanchez-Quevedo et al., 2007; Escamez et al., 2008).

As an important part of the process of evaluation and quality control of the bioengineered tissues, histological analysis must be performed on all tissues generated in the laboratory previously to their clinical implantation in patients (Proussaefs et al., 2002). However, classical histological methods and techniques must be optimized for the novel tissues developed in the laboratory by tissue engineering. In this milieu, handling and processing of native tissues using OCT embedding and cryosection in a cryostat microtome could be a difficult technique even for experienced histotechnologists (Franks, 1998), and no works have been reported on the use of this method on artificial tissues.

In this context, there is a complete lack of information related to the use of classical techniques such as OCT embedding tissue cryosectioning applied to bioengineered human tissues. For that reason, in this work we have carried out an exploratory analysis of the properties and structure of tissues submitted to different methods and incubated in different cryoprotective solutions prior to OCT cryosectioning.

When tissues were tested using several volatile fixing solutions of widespread use in histology and in tissue bank protocols (Holund et al., 1981; Baum et al., 1994) samples presented an inappropriate consistency and the structure of the fiber mesh developed big spaces,

being very different to the paraffin-embedded control samples. For that reason, we can conclude that the use of these compounds is not appropriate for cryosectioning purposes and we therefore suggest that the artificial tissues be embedded in a cryoprotective agent without previous fixation.

In contrast, the use of several types of carbon hydrates, including glucose, maltose and trehalose, resulted in better levels of tissue consistency and appropriate preservation of the tissue structure, especially at certain concentrations and incubation times. Different substances have been used so far as cryoprotective solutions prior to cryofixation of native tissues (Naber et al., 1992; Loken and Demetrick, 2005), especially sucrose (Ljungberg and Johansson, 1993; Whitlon et al., 2001) and trehalose (Norville et al., 2007).

The results of our work demonstrated that preincubation of the bioengineered human tissues in glucose solutions for different times did not result in proper tissue structure preservation. In general, samples preincubated in glucose became partially unstructured, with large empty spaces among the fibers of the scaffold and a large number of artifacts in the slide preparations. For that reason, we conclude that the use of this oligosaccharide is not adequate for tissues intended for *OCT* embedding and cryosectioning.

On the other hand, the use of maltose solutions as cryoprotectant agents for artificial tissues revealed that certain concentrations and incubation times of the different maltose solutions efficiently protected the

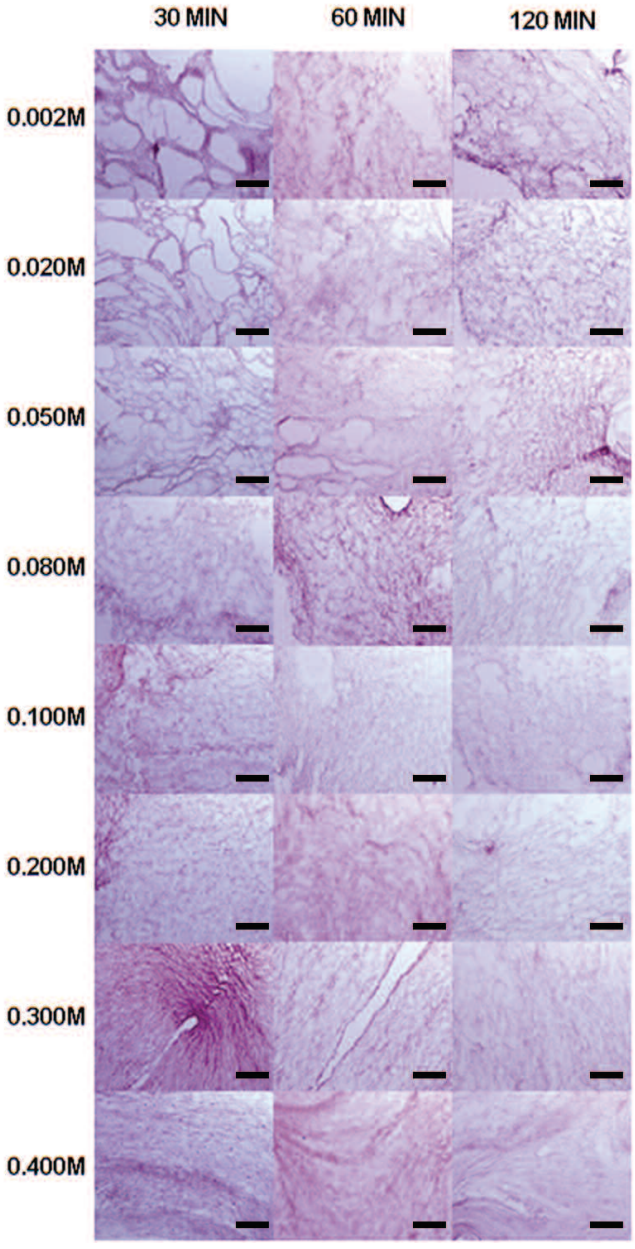


**Fig. 4.** Histological analysis of bioengineered human tissues preincubated in different concentrations of trehalose for 30, 60 or 120 min and embedded in *OCT* for cryosectioning and H&E staining. Scale bars: 1 μm.

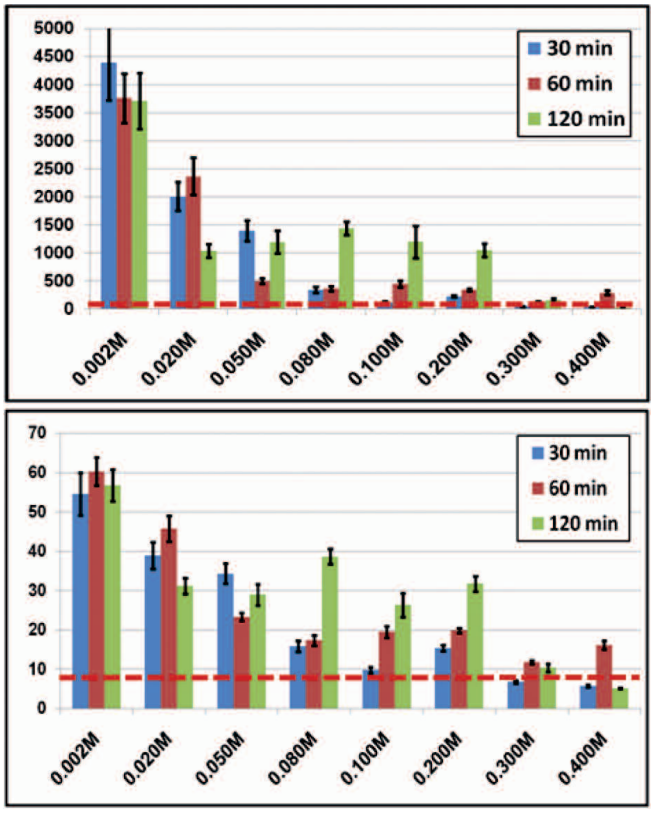


**Fig. 5.** Histograms representing the average areas (top panel) and diameters (lower panels) of samples preincubated in different concentrations of trehalose for different times and embedded in *OCT*. Black bars correspond to standard errors, whereas dotted red lines represent the average area and diameter of control samples embedded in paraffin.

artificial tissues and resulted in histological images that were not significantly different to those obtained by using standard paraffin-embedding techniques. In short, when tissues were incubated in 0.300M and 0.400M maltose solutions for 30 min, we found that the average areas of the interfibrillar spaces of the fiber mesh were 2 to 4 times larger than those found in the control samples, and diameters were around 1.5 fold larger than control samples. These values were clearly lower than those obtained when the artificial tissues were directly embedded in *OCT* and cryosectioned (average areas were 192.7 times higher than control samples and average diameters were 13.3 times higher). In fact, the statistical analysis revealed that the differences with the control were not significant and, therefore, the size of the spaces of the maltose-incubated tissues was comparable to that of control tissues. In contrast, when the artificial tissues were incubated in maltose for 60 min, statistically significant differences with the control tissues were detected at all concentrations, suggesting that this technique was not useful for the processing of the bioengineered tissues. Finally, pretreatment of the human artificial tissues with maltose solutions for 120 min revealed non-significant differences between the control and samples incubated in 0.100M, 0.200M, 0.300M or 0.400M maltose. Of all these concentrations of maltose, 0.400M resulted in small interfibrillar spaces with an average area that was 3.1 times the area of the controls, and a mean diameter of 1.5 times the controls. For that reason, we conclude that the best results using maltose preincubation were found for 120 min and 0.400M concentration of this disaccharide, at least for the kind of tissues used in this work (small pieces of fibrin-agarose scaffolds). To determine the effect of these compounds on artificial tissues of larger volume, it could be necessary to use higher volumes of preincubation solutions. According to previous studies, most of tissues can be efficiently fixed by immersing the samples in a volume of fixing fluid corresponding to at least 25 times the volume of the tissues (Dempster, 1960).

The third carbon hydrate that was tested in this work was disaccharide trehalose. Trehalose can be found in several species with high survival capabilities to dehydration and desiccation, and it has been demonstrated that this carbon hydrate can confer resistance to desiccation and freezing of mammal cells (Guo et al., 2000; Crowe et al., 2001). For that reason, several researchers have used this compound for cryoprotection of samples submitted to cryosectioning for electron crystallographic structure analysis (Hirai et al., 1999) and cryoprotection of freeze-dried native human tissues (Nakamura et al., 2008). Consequently, in this work we hypothesized that trehalose and other related carbon hydrates could protect the bioengineered tissues from damage during the cryofixation, *OCT* embedding and cryosectioning, and therefore improve the biological quality of the analyzed tissues. Our results demonstrated that incubation of the artificial tissues for 30 min in all tested concentrations of trehalose resulted in good tissue quality, especially at the higher concentrations. In fact, statistical comparison of the interfibrillar spaces of controls and tissues incubated in trehalose for 30 min did not show any significant differences, suggesting that the quality of both types of tissues was similar. Strikingly, incubation of the samples for 30 min in 0.300M trehalose resulted in interfibrillar spaces whose area and diameter were virtually identical to those found in paraffin-embedded control samples (no differences were found for the area, whereas diameter of trehalose-pretreated tissues was 0.9 times the diameter of the controls). Similarly, the use of 0.400M trehalose resulted in good tissue quality, with areas and diameters being 0.8 times the area and diameter of the control tissues. Then, if the tissues were incubated in trehalose solutions for 60 min, statistically significant differences were found in comparison to the control for the concentrations of 0.002M and 0.020M, revealing that this technique was not appropriate for tissue cryosectioning. Finally, the results of the tissue preincubation in trehalose for 120 min resulted in very heterogeneous results, with the best results found for 0.300M and 0.400M trehalose. Pretreatment of the tissues with 0.400M trehalose for 120 min was able to efficiently exert cryoprotective functions, and the area and diameter of the interfibrillar spaces found in the tissue were even smaller than those obtained with the use of classical paraffin embedding methods, and no artifacts were generated in the tissues. Due to the fact that samples were not fixed prior to their inclusion in *OCT*, we would propose fixing these tissues immediately after sectioning.

Accordingly, we can conclude that the use of 0.300M or 0.400M trehalose for 30 min is the technique that is able to generate tissue fiber structures that are more similar to the paraffin-embedded control tissues. However, our results suggest that preincubation of the artificial tissues in 0.400M trehalose for 120 min could even improve the quality of the tissues in comparison with the controls. For all those reasons, we would recommend the use of any of these concentrations and incubation times before *OCT* embedding of human artificial tissues.

*Acknowledgements.* This work was supported by the grants FIS PI08/614 from the Spanish Instituto de Salud Carlos III and SAS PI-0132 from Junta de Andalucia.

## References

Alaminos M., Sanchez-Quevedo M.C, Munoz-Avila J.I., Serrano D., Medialdea S., Carreras I. and Campos A. (2006). Construction of a complete rabbit cornea substitute using a fibrin-agarose scaffold. Invest. Ophthalmol. Vis. Sci. 47, 3311-3317.

Alaminos M., Garzon I., Sanchez-Quevedo M.C., Moreu G., Gonzalez-Andrades M., Fernandez-Montoya A. and Campos A. (2007). Time-course study of histological and genetic patterns of differentiation in

human engineered oral mucosa. J. Tissue Eng. Regen. Med. 1, 350-359.

Atala A. (2000). Tissue engineering of artificial organs. J. Endourol. 14, 49-57.

Barthel L.K. and Raymond P.A. (1990). Improved method for obtaining 3-microns cryosections for immunocytochemistry. J. Histochem. Cytochem. 38, 1383-1388.

Baum H.P., Reichrath J., Theobald A. and Schock G. (1994). Fixation requirements for the immunohistochemical reactivity of PCNA antibody PC10 on cryostat sections. Histochem. J. 26, 929-933.

Boland E.D., Telemeco T.A., Simpson D.G., Wnek G.E. and Bowlin G.L. (2004). Utilizing acid pretreatment and electrospinning to improve biocompatibility of poly(glycolic acid) for tissue engineering. J. Biomed. Mater. Res. B Appl. Biomater. 71, 144-152.

Bruder S.P. and Fox B.S. (1999). Tissue engineering of bone. Cell based strategies. Clin. Orthop. Relat. Res. 367 Suppl, S68-83.

Crowe J.H., Crowe L.M., Oliver A.E., Tsvetkova N., Wolkers W. and Tablin F. (2001). The trehalose myth revisited: introduction to a symposium on stabilization of cells in the dry state. Cryobiology 43, 89-105.

Dempster W.T. (1960). Rates of penetration of fixing fluids. Am. J. Anat. 107, 59-72.

Escamez M.J., Carretero M., Garcia M., Martinez-Santamaria L., Mirones I., Duarte B., Holguin A., Garcia E., Garcia V., Meana A., Jorcano J.L., Larcher F. and Del Rio M. (2008). Assessment of optimal virus-mediated growth factor gene delivery for human cutaneous wound healing enhancement. J. Invest. Dermatol. 128, 1565-1575.

Franks J.W. (1998). A precision machine for mounting tissue for Mohs micrographic surgery. Dermatol. Surg. 24, 989-993.

Guo N., Puhlev I., Brown D.R., Mansbridge J. and Levine F. (2000). Trehalose expression confers desiccation tolerance on human cells. Nat. Biotechnol. 18, 168-171.

Hirai T., Murata K., Mitsuoka K., Kimura Y. and Fujiyoshi Y. (1999). Trehalose embedding technique for high-resolution electron crystallography: application to structural study on bacteriorhodopsin. J. Electr. Microsc. (Tokyo) 48, 653-658.

Holund B., Clausen P.P. and Clemmensen I. (1981). The influence of fixation and tissue preparation on the immunohistochemical demonstration of fibronectin in human tissue. Histochemistry 72, 291-299.

Hutmacher D.W., Goh J.C. and Teoh S.H. (2001). An introduction to biodegradable materials for tissue engineering applications. Ann. Acad. Med. Singapore 30, 183-191.

Li W.J., Laurencin C.T., Caterson E.J., Tuan R.S. and Ko F.K. (2002). Electrospun nanofibrous structure: a novel scaffold for tissue engineering. J. Biomed. Mater. Res. 60, 613-621.

Ljungberg A. and Johansson O. (1993). Methodological aspects on immunohistochemistry in dermatology with special reference to neuronal markers. Histochem. J. 25, 735-745.

Loken S.D. and Demetrick D.J. (2005). A novel method for freezing and storing research tissue bank specimens. Hum. Pathol. 36, 977-980.

Moharamzadeh K., Brook I.M., Van Noort R., Scutt A.M. and Thornhill M.H. (2007). Tissue-engineered oral mucosa: a review of the scientific literature. J. Dent. Res. 86, 115-124.

Naber S.P., Smith L.L. Jr and Wolfe H.J. (1992). Role of the frozen tissue bank in molecular pathology. Diagn. Mol. Pathol. 1, 73-79.

Nakamura T., Sekiyama E., Takaoka M., Bentley A.J., Yokoi N., Fullwood N.J. and Kinoshita S. (2008). The use of trehalose-treated freeze-dried amniotic membrane for ocular surface reconstruction. Biomaterials 29, 3729-3737.

Norville J.E., Kelly D.F., Knight T.F. Jr, Belcher A.M. and Walz T. (2007). 7A projection map of the S-layer protein sbpA obtained with trehalose-embedded monolayer crystals. J. Struct. Biol. 160, 313-323.

Proussaefs P., Lozada J., Valencia G. and Rohrer M.D. (2002). Histologic evaluation of a hydroxyapatite onlay bone graft retrieved after 9 years: a clinical report. J. Prosthet. Dent. 87, 481-484.

Rahimi F., Shepherd C.E., Halliday G.M., Geczy C.L. and Raftery M.J. (2006). Antigen-epitope retrieval to facilitate proteomic analysis of formalin-fixed archival brain tissue. Anal. Chem. 78, 7216-7221.

Sanchez-Quevedo M.C., Alaminos M., Capitan L.M., Moreu G., Garzon I., Crespo P.V. and Campos A. (2007). Histological and histochemical evaluation of human oral mucosa constructs developed by tissue engineering. Histol. Histopathol. 22, 631-640.

Whitlon D.S., Szakaly R. and Greiner M.A. (2001). Cryoembedding and sectioning of cochleas for immunocytochemistry and in situ hybridization. Brain Res. Brain Res. Protoc. 6, 159-166.

Accepted July 1, 2009